

Supporting information

Reactive Oxygen Species Activatable Heterodimeric Prodrug as Tumor Selective Nanotheranostics

Meijuan Jiang,^{†‡§} Jing Mu,^{†§*} Orit Jacobson,[§] Zhantong Wang,[§] Liangcan He,[§] Fuwu Zhang,[§] Weijing Yang,[§] Qiaoya Lin,[§] Zijian Zhou,[§] Ying Ma,[§] Jing Lin,[†] Junle Qu,[‡] Peng Huang^{†*} and Xiaoyuan Chen^{§[‡]*}

[†]Marshall Laboratory of Biomedical Engineering, International Cancer Center, Laboratory of Evolutionary Theranostics (LET), School of Biomedical Engineering, Shenzhen University Health Science Center, Shenzhen 518060, China.

[‡]Key Laboratory of Optoelectronic Devices and Systems of Ministry of Education and Guangdong Province, College of Optoelectronic Engineering, Shenzhen University, Shenzhen 518060, China.

[§]Laboratory of Molecular Imaging and Nanomedicine (LOMIN), National Institute of Biomedical Imaging and Bioengineering (NIBIB), National Institutes of Health, Bethesda, Maryland 20892, USA.

[‡]Yong Loo Lin School of Medicine and Faculty of Engineering, National University of Singapore, Singapore, 117597, Singapore.

Schemes, Figures and Tables

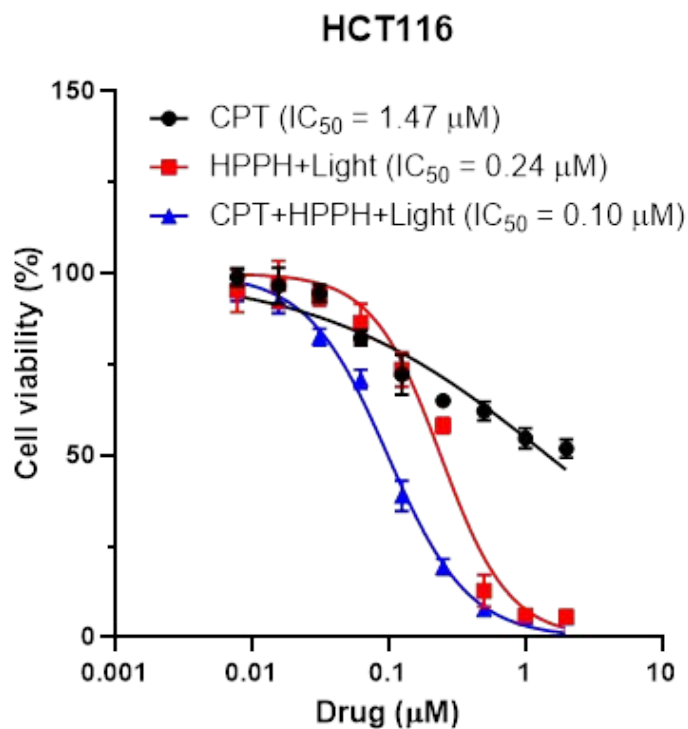
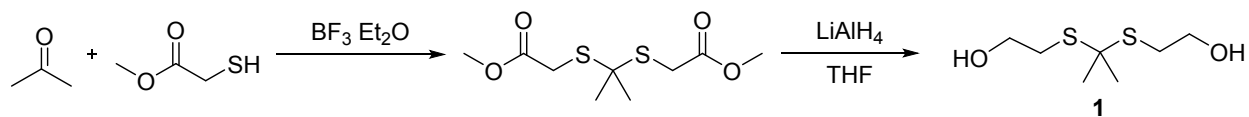


Figure S1. Synergistic therapy of HPPH and CPT. Cell viability of HCT116 cells evaluated by MTT assay. Cells were incubated with CPT, HPPH, CPT+HPPH for 24 h, followed by treatment with/without 671-nm light irradiation (light intensity = 15 mW/cm²) for 5 min and incubated for another 24 h. The combination index was calculated to be 0.49, which is small than 1 and suggests the synergistic effect.



Scheme S1. Synthetic route of **1**.

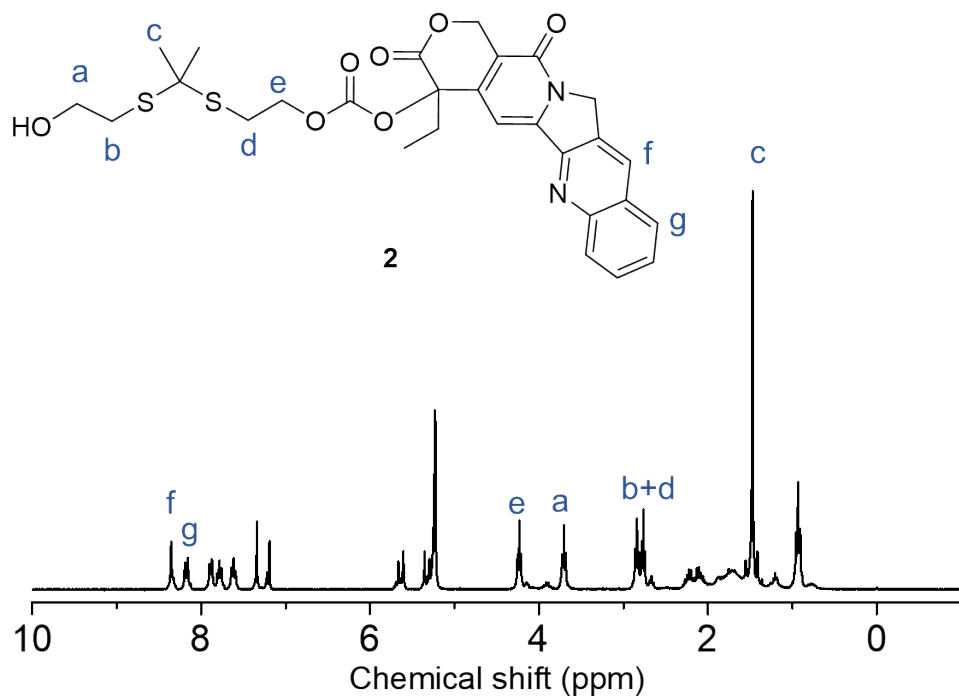


Figure S2. ¹H NMR spectra of CPT prodrug compound 2.

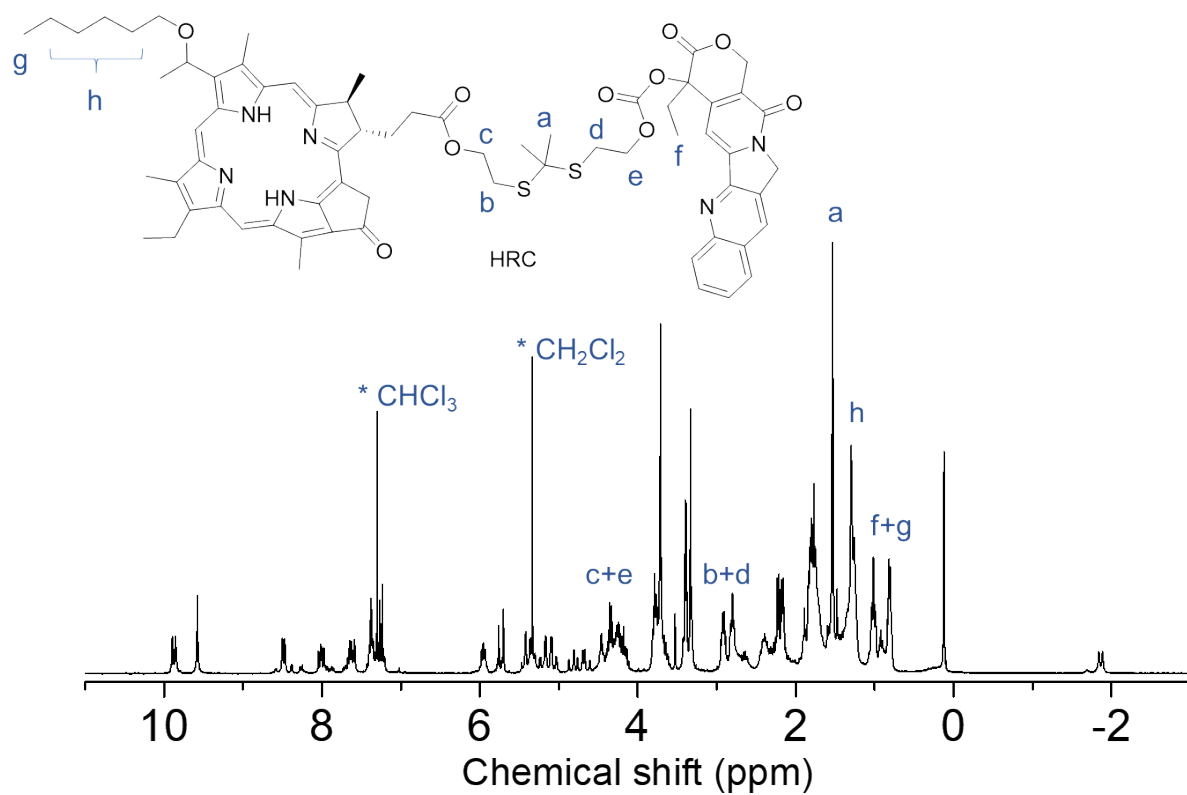


Figure S3. ¹H NMR spectra of HRC. Solvent peaks of CHCl₃, DCM and TMS were noted.

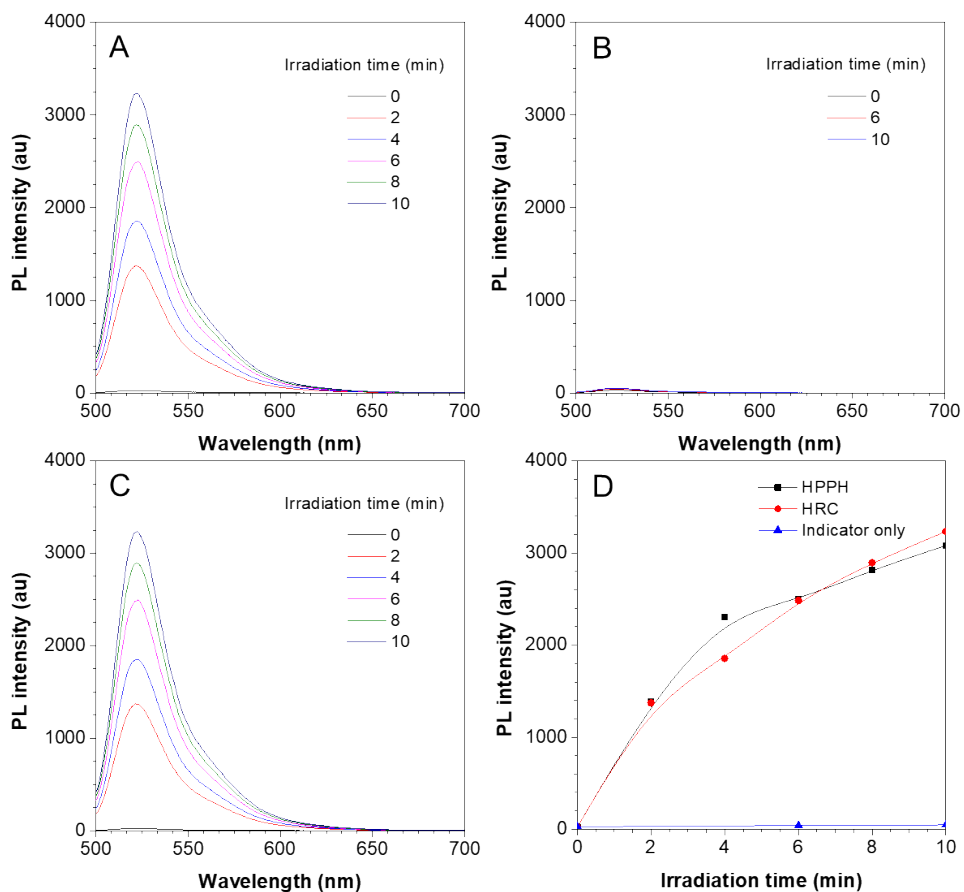


Figure S4. *In vitro* ROS generation using DCFH as ROS indicator. PL spectra of (A) DCFH and HPPH, (B) DCFH only, and DCFH and HRC in PBS under the 671-nm laser irradiation for various time. Concentration of HPPH, HRC or DCFH = 2 μ M. Laser intensity: 100 mW/cm².

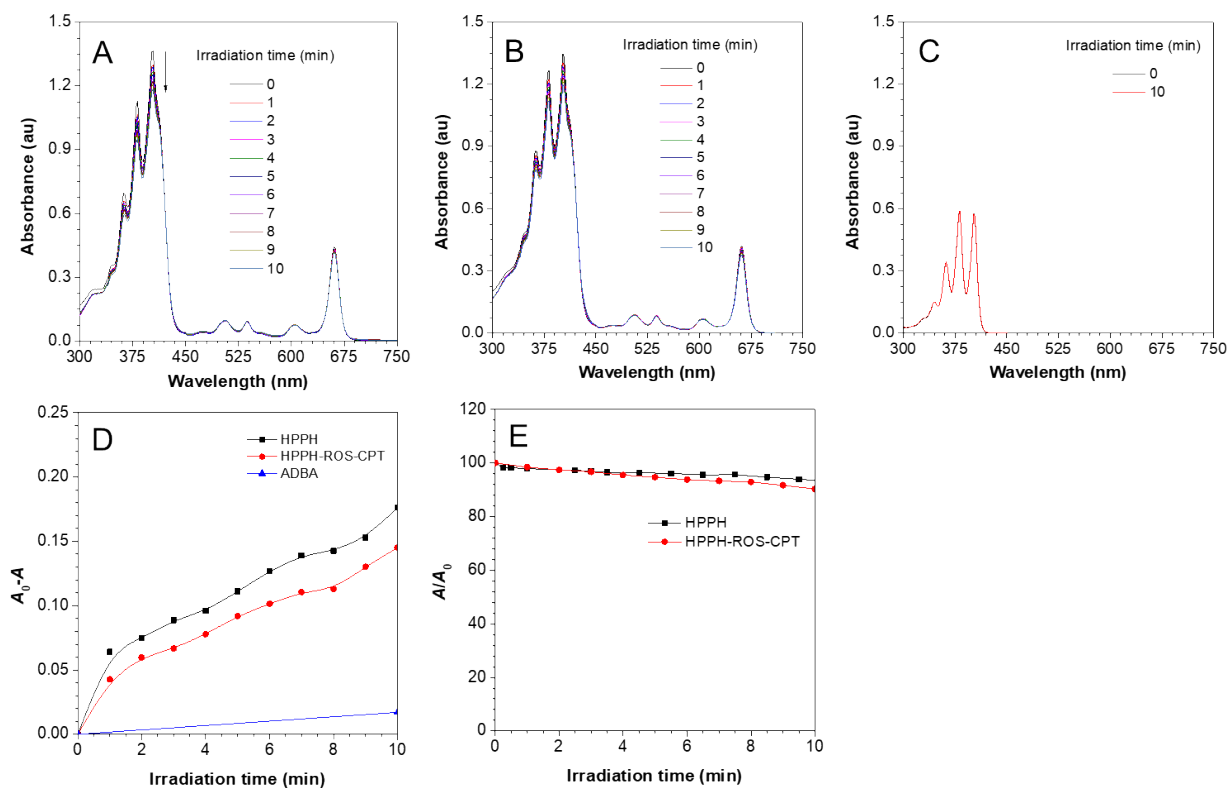


Figure S5. *In vitro* ROS generation determined by 9,10-Anthracenediyl-bis(methylene)dimalonic acid (ADBA). UV-Vis spectra of (A) ADBA and HPPH, (B) ADBA and HRC, (C) ADBA only in DMSO under the 671-nm laser irradiation. Concentration of ADBA = 50 μ M. Concentration of HPPH or HRC = 10 μ M. (D) Absorption change of ADBA at 382 nm upon the laser irradiation in (A), (B) and (C). (E) Photostability of HPPH or HRC determined by the UV-Vis absorption at 660 nm. Laser intensity = 100 mW/cm².

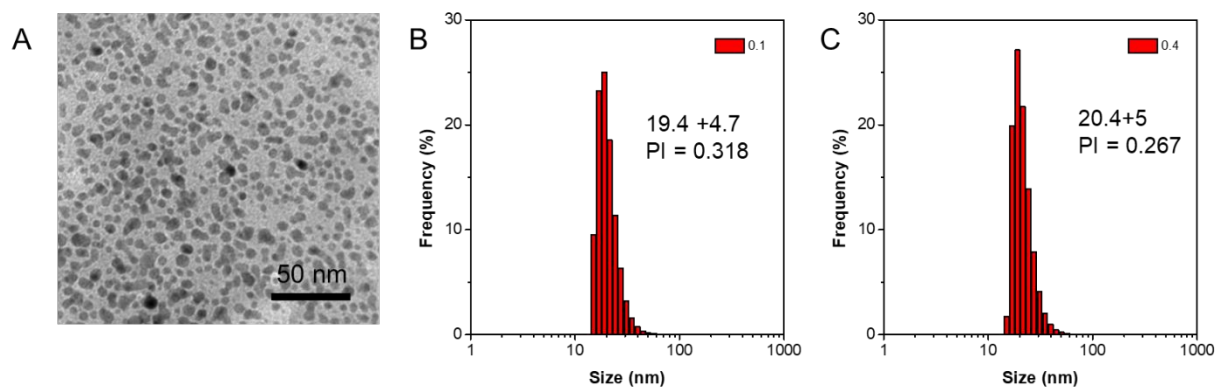


Figure S6. (A) TEM image of HRC@F127 at a drug feeding ratio of 0.2. (B & C) Size distribution analyzed by dynamic laser scattering (DLS) of HRC@F127 with different drug feeding ratios (w/w): (B) 0.1 and (C) 0.4.

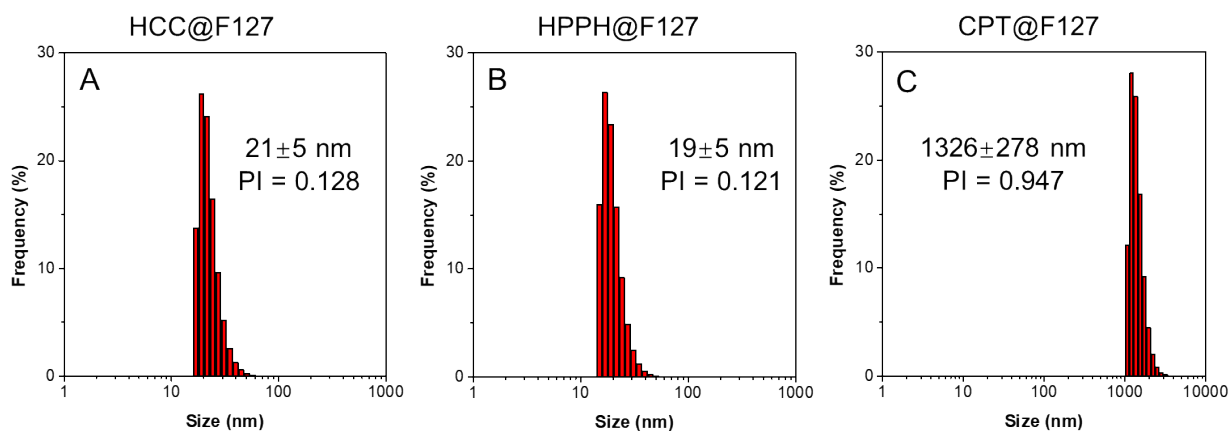


Figure S7. Size distribution analyzed by dynamic laser scattering (DLS) of (A) HCC@F127, (B) HPPH@F127, and (C) CPT@F127.

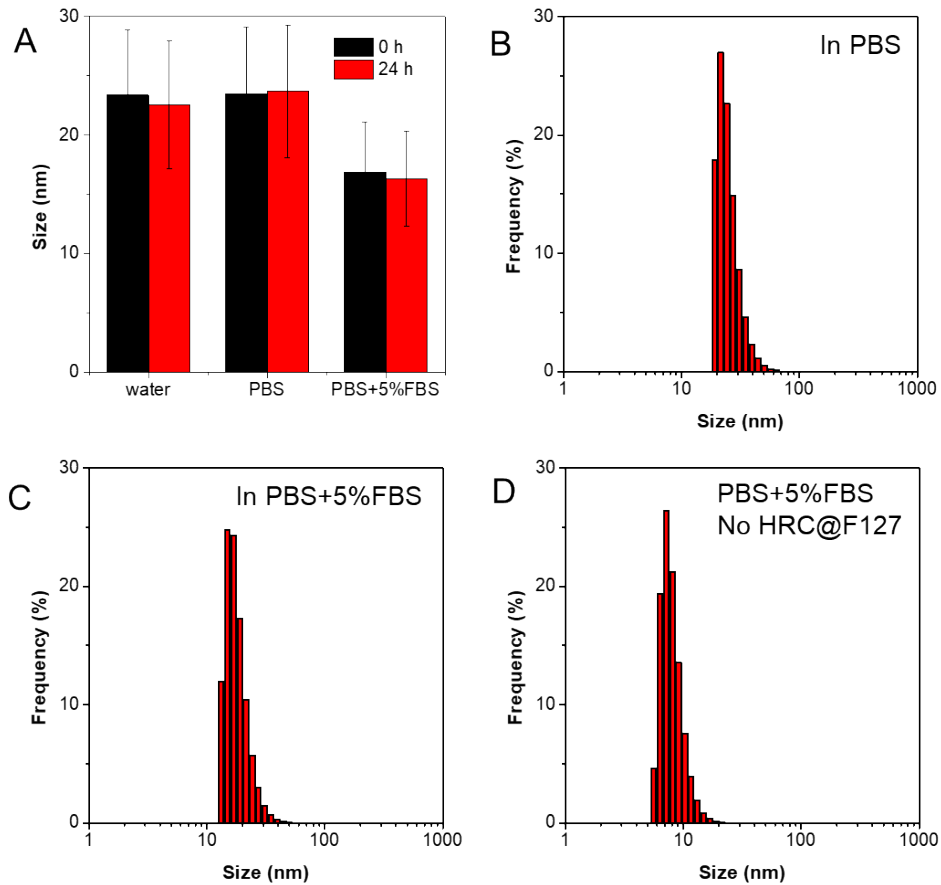


Figure S8. (A) Mean hydrodynamic size distribution of HRC@F127 in water, in PBS and in PBS+5%FBS. (B-D) DLS analysis of hydrodynamic size distribution of (B) HRC@F127 in PBS and (C) HRC@F127 in PBS+5% FBS and (D) no HRC@F127 in PBS+5% FBS. (The smaller hydrodynamic size of HRC@F127 in PBS+5%FBS might be due to the interference of proteins in FBS, which has a mean size of 8 ± 2 nm.)

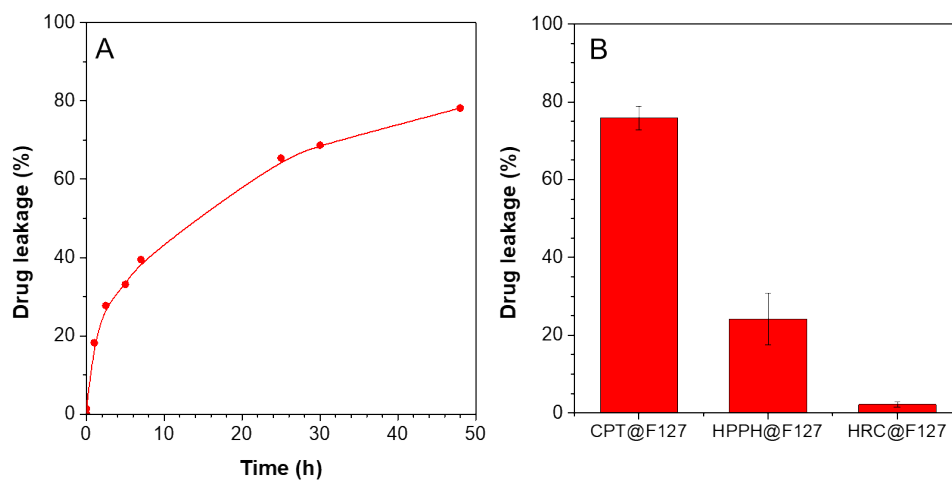


Figure S9. (A) Drug leakage curve of CPT@F127 in PBS *versus* time *via* a dialysis method. (B) Percentage of drug leakage of CPT@F127, HPPH@F127 and HRC@F127 in PBS after incubation for 48 h.

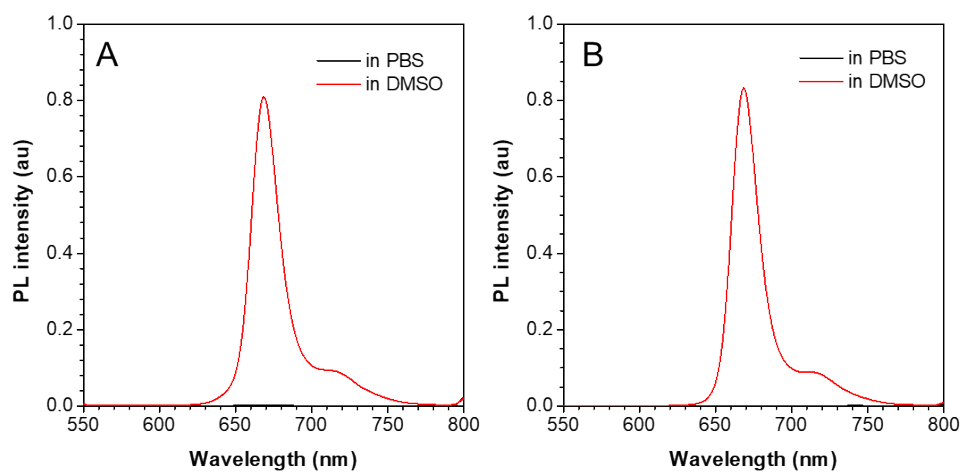


Figure S10. PL spectra of (A) HPPH@F127 and (B) HCC@F127 in PBS and in DMSO. Concentration = 20 μ M.

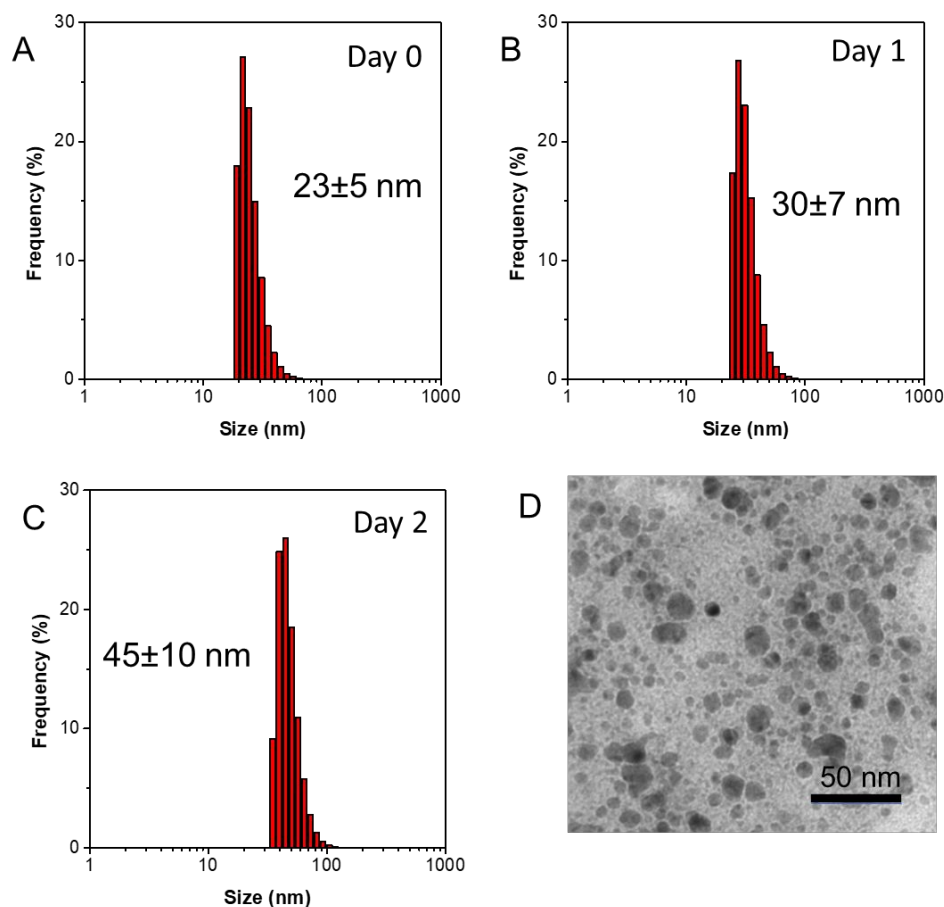


Figure S11. (A–C) DLS analysis of hydrodynamic size distribution of HRC@F127 in water and treated with H_2O_2 for (A) 0 h, (B) 24 h and (C) 48 h. (D) TEM image of HRC@F127 in water and treated with H_2O_2 for 48 h. Scale bar = 50 nm.

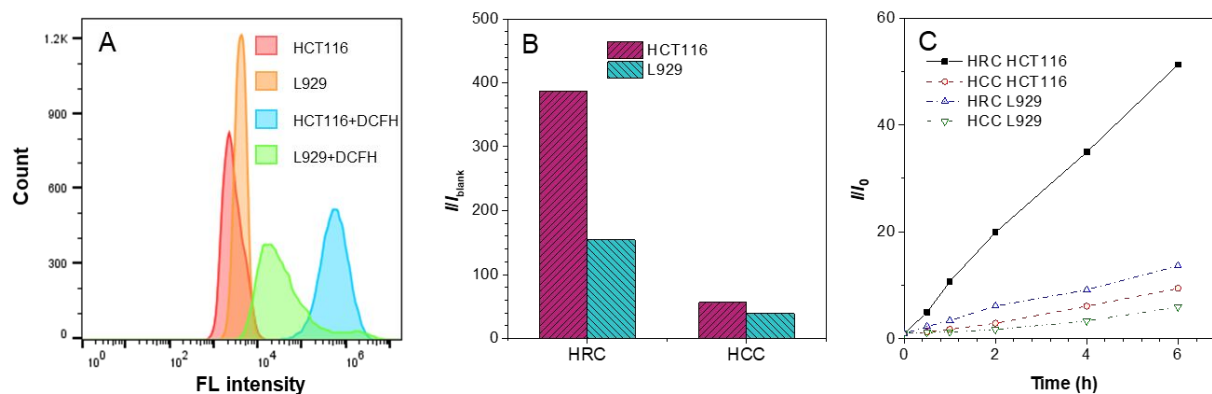


Figure S12. (A) Flow cytometry results of HCT116 cells and L929 cells incubated with/without $5 \mu\text{M}$ DCFH-DA for 1 h. (B) Mean fluorescence intensity of HCT116 and L929 cells incubated with $5 \mu\text{M}$ HRC@F127 or HCC@F127 for 24 hours analyzed by flow cytometry. (C) Mean fluorescence intensity of

HCT116 and L929 cells incubated with 5 μM HRC@F127 or HCC@F127 for various hours analyzed by flow cytometry.

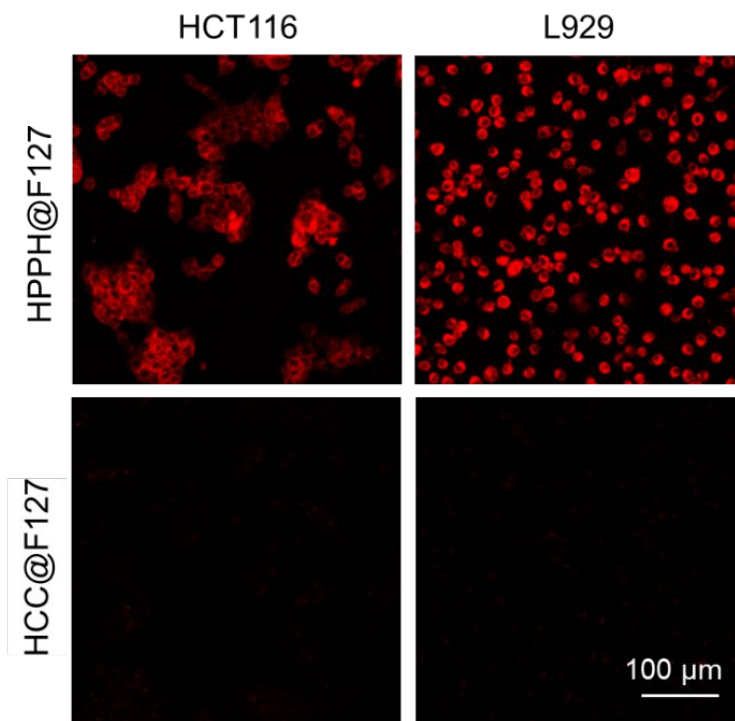


Figure S13. Fluorescence images of HCT116 cells and L929 cells incubated with HPPH@F127 and HCC@F127 for 24 h. Concentration = 5 μM .

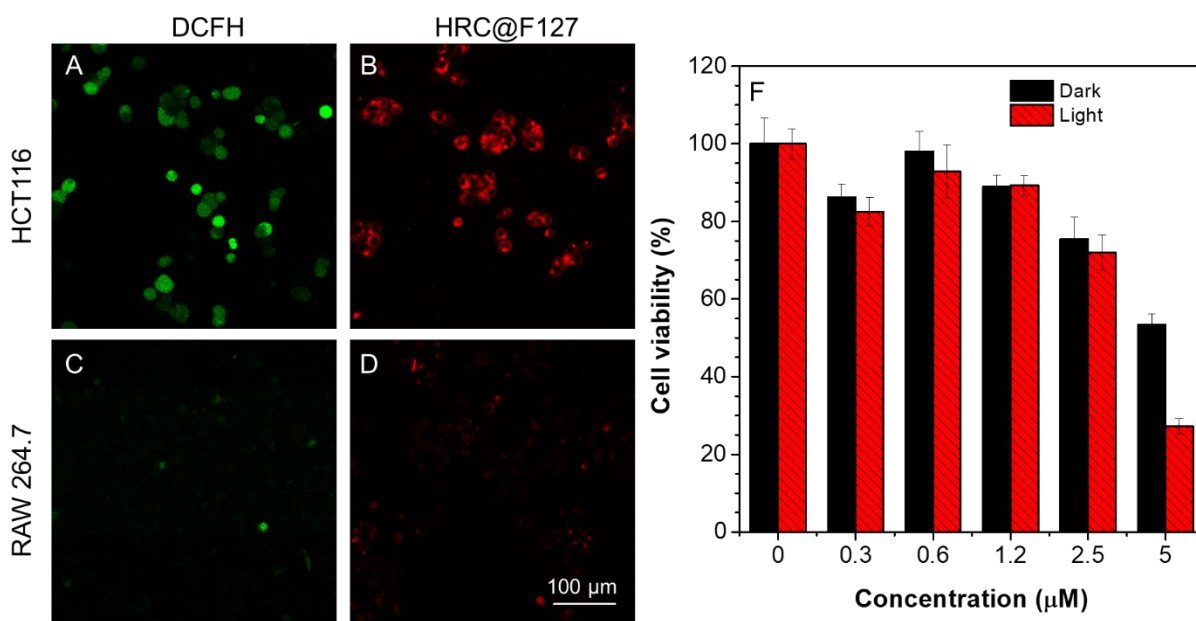


Figure S14. (A–D) Fluorescence images of HCT116 cells and RAW 264.7 cells incubated with 5 μ M DCFH for 1 h or 2 μ M HCC@F127 for 24 h. (F) Cell viability of RAW 264.7 incubated with different concentrations of HRC for 48 h without or with a treatment with 671-nm light irradiation (light intensity = 15 mW/cm²) for 5 min at the time point of 24 h.

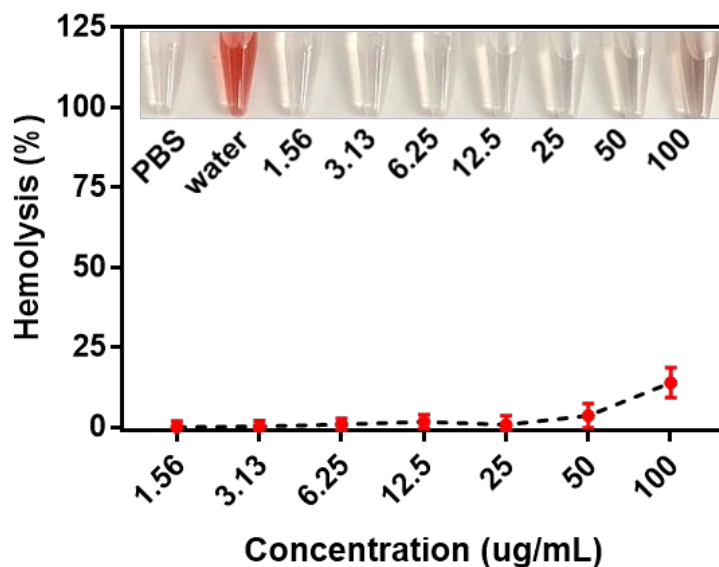


Figure S15. Hemolysis test of HRC@F127 at various concentrations.

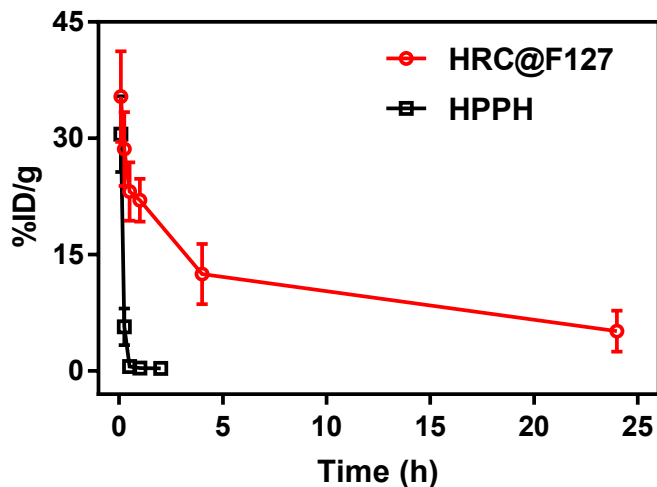


Figure S16. Pharmacokinetics of HRC@F127 and HPPH in mice after intravenous injection. HRC@F127 NPs have a much-prolonged circulation half-life ($t_{1/2} = 1.6$ h) than HPPH molecules ($t_{1/2} = 0.1$ h).

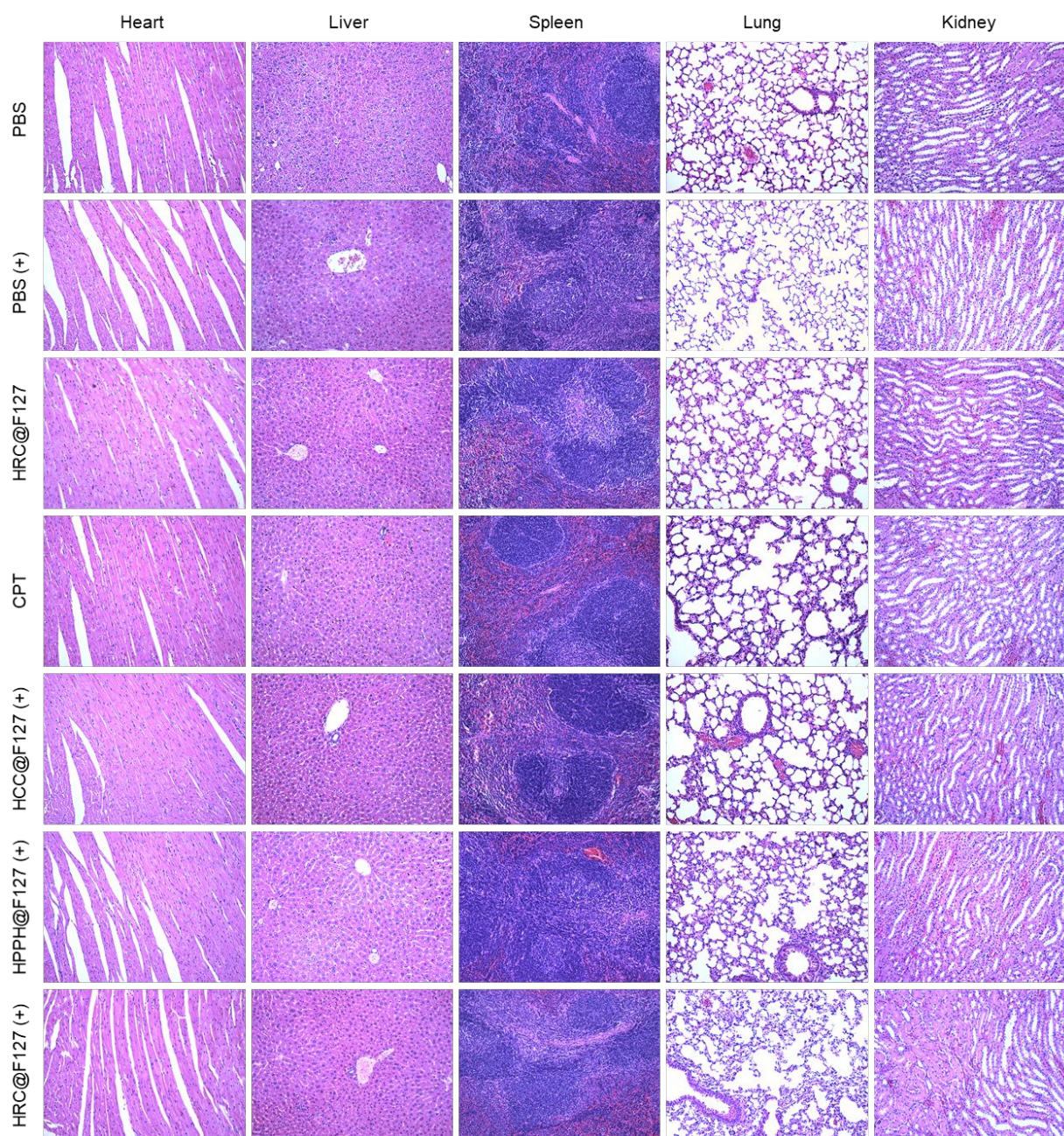


Figure S17. Hemotoxylin and Eosin (H&E) staining images of major organs in HCT116 tumor-bearing mice treated with specified regimens: G1 (PBS), G2 (PBS + Laser), G3 (HRC@F127), G4 (CPT), G5 (HCC@F127 + Laser), G6 (HPPH@F127 + Laser), and G7 (HRC@F127 + Laser).

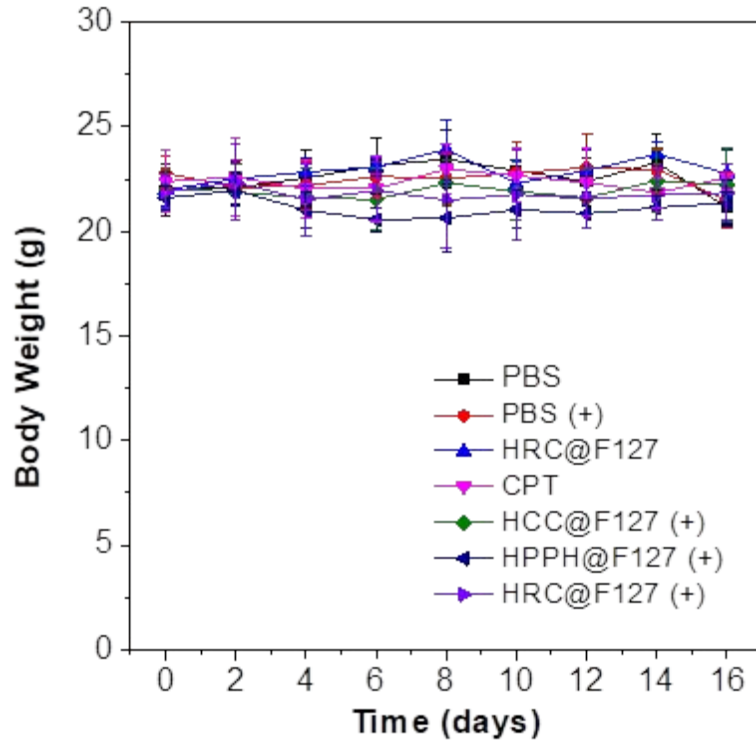


Figure S18. Change of body weight of HCT116 tumor-bearing mice with time after treated with specified regimens: G1 (PBS), G2 (PBS + Laser), G3 (HRC@F127), G4 (CPT NPs), G5 (HCC@F127 + Laser), G6 (HPPH NP + Laser), and G7 (HRC@F127 + Laser).